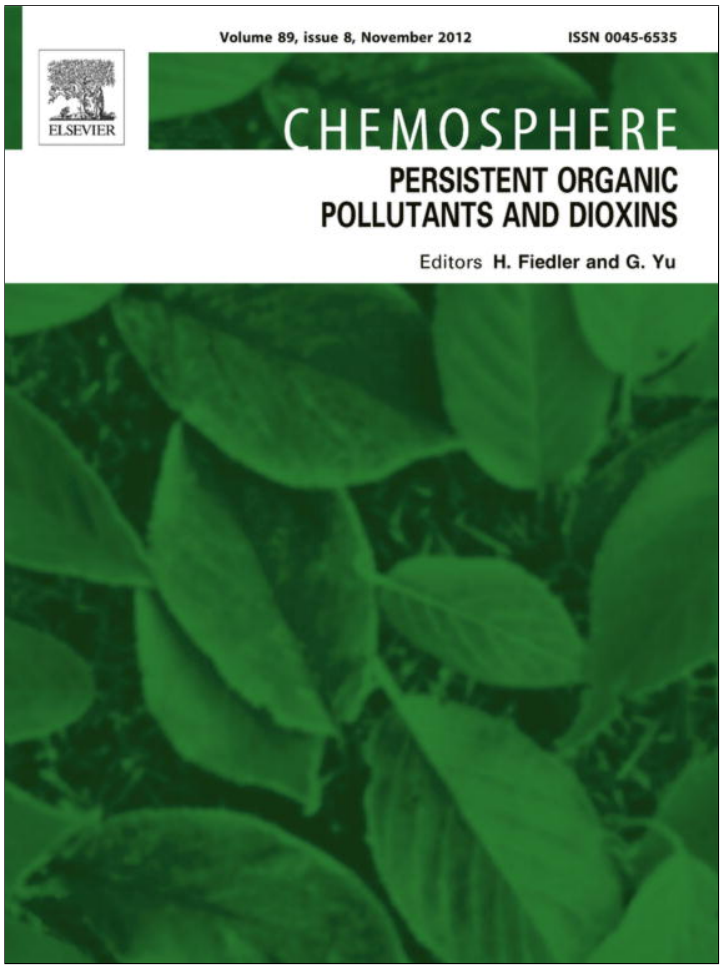

Chemosphere 89 (2012) 950–956

Contents lists available at SciVerse ScienceDirect

Chemosphere

journal homepage: www.elsevier.com/locate/chemosphere

The oxidation mechanism of polychlorinated dibenzo-*p*-dioxins under the atmospheric conditions – A theoretical study

Liming Wang *, Aili Tang

School of Chemistry & Chemical Engineering, South China University of Technology, Guangzhou 510640, China

HIGHLIGHTS

- The atmospheric oxidation mechanisms of PCDDs are different from those of benzene.
- Initial OH addition to PCDDs occur mainly on the γ-sites.
- Predicted rate constants for OH addition to PCDDs agree reasonably with experiment.
- PCDD-γ-OH adducts undergo fused-ring C–O cleavage.
- 2,3,7,8-TCDDs will be converted to substituted phenoxy radicals.

GRAPHICAL ABSTRACT

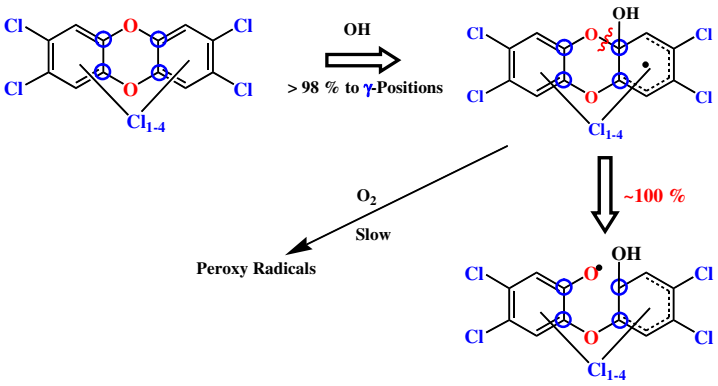

ARTICLE INFO

Article history:
Received 13 October 2011
Received in revised form 22 May 2012
Accepted 30 June 2012
Available online 24 July 2012

Keywords:
Dibenzo-*p*-dioxins
Atmospheric oxidation mechanism
Potential Energy Surfaces
PCDD-OH adducts

ABSTRACT

The atmospheric polychlorinated dibenzo-*p*-dioxins (PCDDs) partition appreciably in the gas phase, where they undergo rapid oxidation. The atmospheric oxidation mechanisms of a few PCDDs, initiated by OH radical, are studied using density functional theory calculations. The oxidations start with OH-addition to the aromatic rings, dominantly at γ-sites, followed by the non-chlorinated β-sites; while additions to the α-sites or chlorinated sites are negligible. For PCDDs with all β-sites being chlorinated, formation of PCDD-γ-OH adducts become virtually the only reaction path. Under the atmospheric conditions, the PCDD-β/γ-OH adducts combine with O_2 slowly at rates <1 s^{-1}. Instead, the PCDD-β-OH adducts will react with O_2 through hydrogen abstraction at rates <50 s^{-1}, forming PCDD-β-ol, and the PCDD-γ-OH adducts will decompose to the substituted phenoxy radicals by fused-ring C–O bond cleavage at rates of $10^3 \sim 10^5$ s^{-1}. The reaction mechanisms of PCDDs are drastically different from the peroxy mechanism for the atmospheric oxidations of benzene and dibenzofuran.

1. Introduction

Polychlorinated dibenzo-*p*-dioxins and dibenzofurans (PCDD/Fs) are notorious pollutants being emitted primarily from waste incinerators (Brubaker and Hites, 1998). Even though PCDD/Fs partition mostly in soil and sediments in the environment, atmospheric transport represents the primary distribution pathway moving PCDD/Fs from the emission sources to terrestrial and aquatic ecosystems. The vapor pressures of PCDD/Fs are from 10^{-1} to 10^{-8} Pascal at 298 K (Eitzer and Hites, 1988; Song et al., 2001; Mader and Pankow, 2003). Because of the extremely low PCDD/Fs concentrations from a few fg m^{-3} to hundreds pg m^{-3} in the atmosphere (Hippelein et al., 1996; Lee et al., 1999; Li et al., 2008a, 2008b; Zhang et al., 2009), both field measurements and model predictions found appreciable partition of PCDD/Fs in the gas phase, even for the low volatile Hepta-/Octa-CDD/F congeners (Nakano et al., 1990; Kaupp and McLachlan, 1999; Lohmann et al., 2000;

* Corresponding author. Tel.: +86 20 87112900; fax: +86 20 87112906.
E-mail address: wanglm@scut.edu.cn (L. Wang).

0045-6535/$ - see front matter © 2012 Elsevier Ltd. All rights reserved.
http://dx.doi.org/10.1016/j.chemosphere.2012.06.050

Handy and Cohen, 2001; Chao et al., 2004; Bylaska et al., 2006; Lee et al., 2008; Ohura et al., 2008; Hofzumahaus et al., 2009). During transport, the gas phase PCDD/Fs can be removed by reactions or deposition (Atkinson, 2001). Comparison of the homologue profiles for PCDD/Fs between combustion sources and environmental sinks clearly shows the removal of PCDD/Fs during their atmospheric transport for congeners with four to seven chlorine substitutions (Brzuzy and Hites, 1996; Brubaker and Hites, 1998). Field measurements across the United Kingdom and Ireland also revealed the depletion of PCDD/Fs during the transport (Lohmann et al., 1999).

The depletion of gaseous PCDD/Fs during the atmospheric transport is mainly due to their reactions with OH radical, while wet and dry depositions of the gaseous PCDD/Fs are of minor importance (Shih et al., 2006; Valsaraj and Thibodeaux, 2010). Reactions with NO_3, O_3, and HO_2 and photodegradation are also slow (Sinkkonen and Paasivirta, 2000). There have been a few kinetic studies on the reactions of PCDDs with OH radical, obtaining the bimolecular rate coefficients in the range of $10^{-12} \sim 10^{-10}$ $cm^3\ mol^{-1}\ s^{-1}$ at ~298 K and atmospheric lifetimes of hours to days for different congeners (Kowk et al., 1994, 1995; Brubaker and Hites, 1998; Bylaska et al., 2006). The reactions are believed to start with the OH addition to the aromatic rings.

There have also been a few theoretical studies on the oxidation mechanism of PCDD/Fs. Lee et al. (2004) found that OH radical added dominantly to the γ-site for reactions of DD, 1,4,6,9- and 2,3,7,8-TCDDs using density functional theory (DFT) calculations. They also assumed that the radical adducts will combine immediately with the atmospheric O_2, in analogy to the reaction mechanisms of benzene and toluene with OH radical (Calvert et al., 2002). Zhang et al. (2011) predicted the rates of O_2 addition to 2,3,7,8-TCDD-γ-OH adduct, and suggested that TCDD-OH-O_2 will react with NO or H_2O. However, our recent study on DD and 2,3,7,8-TCDD showed that the (TC)DD-γ-OH adducts will undergo fused-ring C–O breakage instead of reacting with O_2 under the atmospheric conditions, assuming rate constants of DD-OH + O_2 are similar to those of DF-OH + O_2 (Wang and Tang, 2011). Theoretical study on oxidation mechanism of dibenzofuran (DF) predicted similar mechanism and suggested the formation of 1-dibenzofuranol from DF-1-OH + O_2 under the atmospheric conditions (Altarawneh et al., 2008). Here, we extended our theoretical study to six symmetric Di-CDDs, 1,4,6,9-Tetra-CDD, and Octa-CDD to obtain a better understanding on the oxidation mechanism of PCDDs.

2. Computational methods

All DFT calculations are carried out by using Gaussian 03 suite of programs (Frisch et al., 2004). Geometries are optimized and the vibrational frequencies are evaluated at B3LYP/6-311++G(2df,p) level, and are used for computing the thermodynamic parameters. Rate constants are estimated using the traditional transition state theory (TST) as (Pilling and Seakins, 1999):

$$k_b = \frac{k_B T}{h} \cdot \exp\left(-\frac{\Delta_r G^{\neq}_{298K}}{RT}\right) \cdot \frac{RT}{P^{\circ}} \cdot \frac{10^6}{N_A} \quad \text{(E1)}$$

for bimolecular rate constants k_b (in $cm^3\ mol^{-1}\ s^{-1}$) and

$$k_{Uni} = \frac{k_B T}{h} \cdot \exp\left(-\frac{\Delta_r G^{\neq}_{298K}}{RT}\right) \quad \text{(E2)}$$

for high-pressure-limit unimolecular rate constant k_{Uni} (in s^{-1}), where k_B is the Boltzmann constant. Table S1 of Supporting Information (SI) lists the zero-point energy corrections, electronic energies, and Gibbs free energies, from which the reaction energetics ($\Delta_r H$ and $\Delta_r G$) are obtained.

Better predictions for the rate constants can be achieved using variational TST, which, however, requires the detailed and burdensome knowledge of the potential energy surface over an extended range of reaction coordinates near the transition states. Tunneling

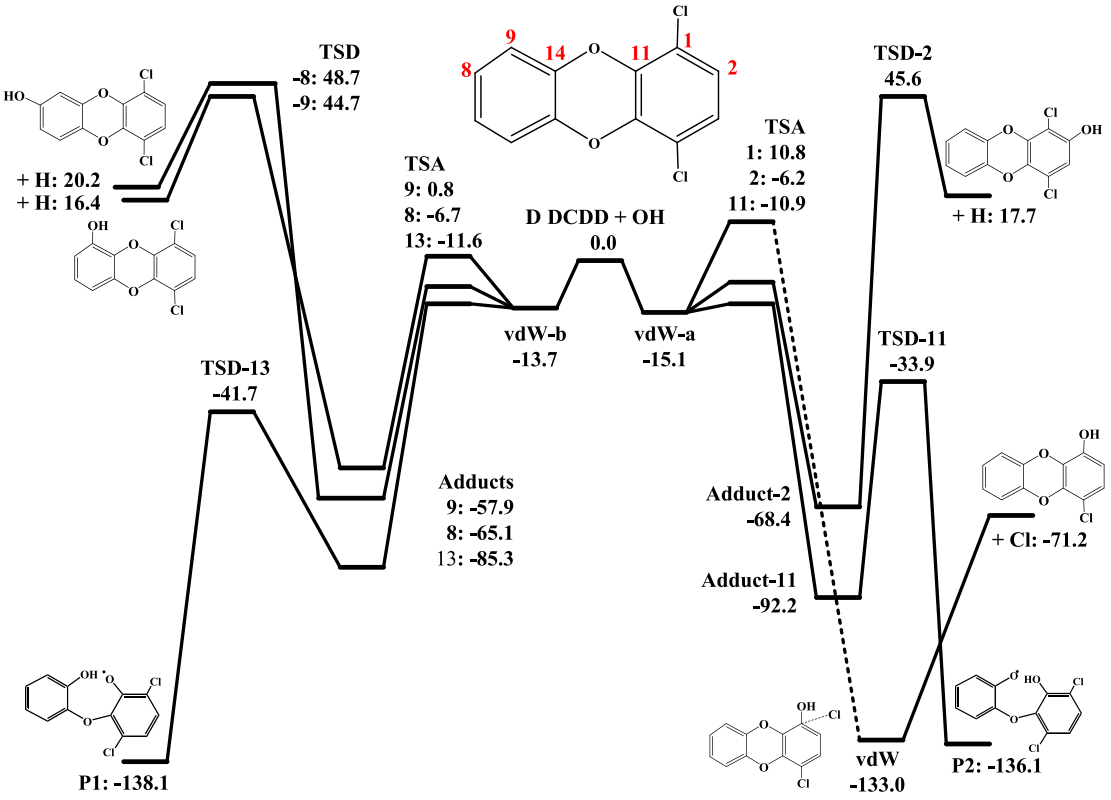

Fig. 1. The potential energy diagram for 1,4-Di-CDD + OH ($\Delta_r H_{0K}$, in kJ mol^{-1}).

effect is also ignored here because of the small curvature near the saddle point as evidenced by the small imaginary frequencies associated with the OH additions, e.g., 259*i* cm^{-1} for OH addition to C_2 of 1,4,6,9-TCDD. Given the relatively large uncertainty of DFT methods, detailed treatments on variational and tunneling effects are unlikely to significantly improve the estimated rate constants. Despite the uncertainties, the predicted reaction pathways are still reasonably valid because of the large differences on barrier heights between different channels.

3. Results and discussion

3.1. PCDD-OH adduct formation

The atmospheric oxidation of PCDDs begins with the OH addition to the aromatic rings, forming PCDD-OH adducts. The OH addition can occur at three different positions (C_α, C_β, C_γ) for DD, 2,3,7,8-/1,4,6,9-TCDD, and OCDD, and six positions for DCDDs. Typical structures for reaction of 1,4,6,9-TCDD are shown in Fig. S1. Pre-reactive van der Waals (vdW) complexes are found between all PCDDs and OH radical.

Thermodynamics for the formations of vdW complexes and adducts between PCDDs and OH radical are given in Table S2, and the typical potential energy diagram is shown in Fig. 1 for reaction of 1,4-DCDD (Figs. S3–S9 in SI for others). All adducts are thermodynamically stable relative to the reactants. Addition of OH to the chlorinated carbon positions results in substitution, forming complexes between dibenzo-*p*-dioxinol (PCDD-ol) and chlorine atom, e.g., the OH addition to C_α of 1,4,6,9-TCDD (Fig. S1). Similar substitution and complex structure were also found for reaction between chlorobenzene and OH (Bryukov et al., 2009). Nevertheless, the additions to the chlorinated carbon position have barriers much higher than the ones to other non-chlorinated positions.

For the non-chlorinated positions, the additions to the C_γ are the most exothermic, e.g., the stabilization energies ($\Delta_r H^0_{0K}$) of −66.3, −58.2, and −82.3 kJ mol^{-1} for DD-α-OH, DD-β-OH, and DD-γ-OH, respectively. The B3LYP/6-311++G(2df,p) stabilization energies of DD-α-OH and DD-β-OH are close to that of −57.4 kJ mol^{-1} for the C_6H_6-OH adduct, which in turn agrees closely with the value of −55.2 kJ mol^{-1} at high level of modified Gaussian-2

Table 1
Rate constants (k_b in $cm^3\ mol^{-1}\ s^{-1}$), branch ratios (Γ), and the estimated atmospheric half-lives due to reaction with OH radicals (in **black**, in hours, assuming [OH] ~ 10^6 mol cm^{-3}) for OH addition to PCDDs.

PCDDs/Adducts[a]	$k_{b,298K}$[b]	Γ or $t_{1/2}$	Reactions[a]	$k_{b,298K}$[b]	Γ or $t_{1/2}$
DD			1,4,6,9-TCDD		
DD-1-α-OH	7.95×10^{-13}	0.011	1,4,6,9-TCDD-1-α-OH	3.23×10^{-15}	0.000
DD-2-β-OH	3.03×10^{-11}	0.422	1,4,6,9-TCDD-2-β-OH	3.63×10^{-12}	0.229
DD-11-γ-OH	4.07×10^{-11}	0.567	1,4,6,9-TCDD-11-γ-OH	1.23×10^{-11}	0.771
Overall (Calc.)	7.18×10^{-11}	**2.7 h**	Overall (Calc.)	1.59×10^{-11}	**12.1 h**
Overall (Expt.)[c]	4.58×10^{-11}				
Overall (Expt.)[d]	$(1.1 \sim 1.4) \times 10^{-11}$				
Overall (Expt.)[e]	$(1.48 \pm 0.35) \times 10^{-11}$				
2,3,7,8-TCDD			OCDD		
2,3,7,8-TCDD-1-α-OH	4.62×10^{-13}	0.015	OCDD-1-α-OH	3.37×10^{-15}	0.000
2,3,7,8-TCDD-2-β-OH	9.74×10^{-15}	0.000	OCDD-2-β-OH	5.30×10^{-15}	0.000
2,3,7,8-TCDD-11-γ-OH	3.08×10^{-11}	0.985	OCDD-11-γ-OH	2.04×10^{-11}	1.000
Overall (Calc.)	3.12×10^{-11}	**6.2 h**	Overall (Calc.)	2.04×10^{-11}	**9.4 h**
			Overall (Expt.)[c]	0.34×10^{-11}	
1,4-DCDD			2,3-DCDD		
1,4-DCDD-2-β-OH	4.05×10^{-12}	0.139	2,3-DCDD-1-α-OH	3.88×10^{-13}	0.010
1,4-DCDD-8-β-OH	5.12×10^{-12}	0.176	2,3-DCDD-2-β-OH	1.04×10^{-14}	0.000
1,4-DCDD-9-α-OH	1.92×10^{-13}	0.007	2,3-DCDD-8-β-OH	5.92×10^{-12}	0.151
1,4-DCDD-11-γ-OH	8.53×10^{-12}	0.293	2,3-DCDD-9-α-OH	1.91×10^{-13}	0.005
1,4-DCDD-14-γ-OH	1.12×10^{-11}	0.385	2,3-DCDD-11-γ-OH	1.69×10^{-11}	0.430
Overall (Calc.)	2.91×10^{-11}	**6.6 h**	2,3-DCDD-14-γ-OH	1.59×10^{-11}	0.404
			Overall (Calc.)	3.93×10^{-11}	**4.9 h**
			Overall (Expt.)[c]	2.21×10^{-11}	
1,6-DCDD			2,7-DCDD		
1,6-DCDD-1-α-OH	4.00×10^{-16}	0.000	2,7-DCDD-1-α-OH	3.49×10^{-13}	0.006
1,6-DCDD-2-β-OH	6.57×10^{-12}	0.223	2,7-DCDD-2-β-OH	4.99×10^{-15}	0.000
1,6-DCDD-3-β-OH	2.27×10^{-12}	0.077	2,7-DCDD-3-β-OH	7.29×10^{-12}	0.116
1,6-DCDD-4-α-OH	6.29×10^{-13}	0.021	2,7-DCDD-4-α-OH	1.30×10^{-13}	0.002
1,6-DCDD-11-γ-OH	1.39×10^{-11}	0.472	2,7-DCDD-11-γ-OH	1.02×10^{-11}	0.162
1,6-DCDD-12-γ-OH	6.10×10^{-12}	0.207	2,7-DCDD-12-γ-OH	4.47×10^{-11}	0.714
Overall (Calc.)	2.95×10^{-11}	**6.5 h**	Overall (Calc.)	6.26×10^{-11}	**3.1 h**
			Overall (Expt.)[c]	0.74 × 10–11	
1,9-DCDD			2,8-DCDD		
1,9-DCDD-1-α-OH	4.77×10^{-16}	0.000	2,8-DCDD-1-α-OH	2.89×10^{-13}	0.005
1,9-DCDD-2-β-OH	7.07×10^{-12}	0.219	2,8-DCDD-2-β-OH	5.86×10^{-15}	0.000
1,9-DCDD-3-β-OH	3.07×10^{-12}	0.095	2,8-DCDD-3-β-OH	6.91×10^{-12}	0.124
1,9-DCDD-4-α-OH	7.03×10^{-13}	0.022	2,8-DCDD-4-α-OH	1.62×10^{-13}	0.003
1,9-DCDD-11-γ-OH	1.27×10^{-11}	0.392	2,8-DCDD-11-γ-OH	9.99×10^{-12}	0.179
1,9-DCDD-12-γ-OH	8.82×10^{-12}	0.273	2,8-DCDD-12-γ-OH	3.84×10^{-11}	0.689
Overall (Calc.)	3.24×10^{-11}	**6.0 h**	Overall (Calc.)	5.57×10^{-11}	**3.5 h**
			Overall (Expt.)[c]	0.71×10^{-11}	

[a] Values for DD and 2,3,7,8-TCDD are from Wang and Tang (Wang and Tang, 2011).
[b] Bimolecular rate constants are calculated using traditional transition state theory (Eq. (E1)).
[c] From Taylor et al. (2005).
[d] From Brubaker and Hites (1998).
[e] From Kowk et al. (1994).

(Tokmakov and Lin, 2002). Therefore, no effort is undertaken to refine the reaction energies for OH additions to PCDDs using the isodesmic reactions which have been used in previous studies (Lee et al., 2004; Altarawneh et al., 2008; Bryukov et al., 2009).

Also listed in Table S2 are the barrier heights for OH addition to PCDDs. Negative barriers are found for additions to all the C_γ and to some of the non-chlorinated C_α and C_β, and this can obviously be accounted for by the existence of pre-reactive vdW complexes which are below PCDD + OH by 13 ~ 16 kJ mol^{-1} (Table S2). The negative barriers are consistent with the experimental activation energies of −0.29 ± 0.49 kJ mol^{-1} (Brubaker and Hites, 1998) and of −8.1 ± 0.5 kJ mol^{-1} (Bylaska et al., 2006) for DD + OH, and of −6.2, −4.7, and −4.8 kJ mol^{-1} for 2,3-, 2,7-, and 2,8-Di-DDs, but is contrast to the experimental activation energy of 5.5 kJ mol^{-1} for Octa-CDD + OH (Bylaska et al., 2006).

Table 1 lists the estimated bimolecular rate constants using thermodynamic parameters given in Table S2. The calculated $k_{b,298K}$ for OH additions to DD, 2,3-Di-CDD, 2,7-Di-CDD, 2,8-Di-CDD, and Octa-CDD are 7.18, 3.93, 6.26, 5.57, and 2.04 × 10^{-11} cm^3 mol^{-1} s^{-1}, all being in reasonable agreement with the experimental values of (1.2 ± 0.3) and 4.6 × 10^{-11} cm^3 mol^{-1} s^{-1} for DD (Brubaker and Hites, 1998; Bylaska et al., 2006) and of 2.21, 0.74, 0.71, and 0.34 × 10^{-11} cm^3 mol^{-1} s^{-1} for the others (Bylaska et al., 2006), respectively, though the predicted values for 2,7-Di-CDD, 2,8-Di-CDD, and Octa-CDD are 7 ~ 9 times higher. This is probably due to the well-known factor that B3LYP tends to underestimate the barrier heights (Zhao and Truhlar, 2005), albeit no aromatic molecules were included in the evaluation reaction set. Nevertheless, the agreement between the traditional TST predictions and measurements is reasonable and acceptable, due probably to the canceling of errors.

Branch ratios for additions to different carbons are also predicted (Table 1). The prediction of branch ratios should be more reliable than the predictions for the absolute rate constants because it depends mainly on the relative barrier heights between different channels (see Eq. (E1)). The additions to C_γ are favored kinetically over those to C_α and C_β, agreeing with the previous studies (Lee et al., 2004; Wang and Tang, 2011). For all PCDDs, additions to the chlorinated carbon sites are negligible because of their much higher barriers than others, as for the addition of OH to chlorobenzene (Bryukov et al., 2009). Additions to non-chlorinated C_α are also of minor importance, usually accounting for less than 1% of branch ratio and maxima of ~2% for addition to $C_{4\alpha}$ site for 1,6/1,9-DCDDs (Table 1). Therefore, the OH reaction with PCDDs is dominated by C_γ-addition, followed by addition to the non-chlorinated C_β. For 2,3,7,8-PCDDs (all C_β being chlorinated), formation of PCDD-γ-OH adducts are expected to be almost 100%. For PCDDs with non-chlorinated C_β, formations of PCDD-γ-OH adducts still dominate over those of PCDD-β-OH, e.g., branch ratios of 31.5% and 30.0% for 1,4-DCDD-β-(2 + 8)-OH and 1,6-DCDD-β-(2 + 3)-OH, respectively.

The calculated rate constants are in the range of 10^{-11} to 10^{-10} cm^3 mol^{-1} s^{-1}, rendering the half-lives ($t_{1/2} = \ln 2/k_b$[OH]) of gaseous PCDDs in the range of 2 ~ 12 h, assuming [OH] ~ 10^6 mol cm^{-3} in the atmosphere. This indicates that most of the gaseous PCDDs will be degraded during their long range transport, and the persistency of Octa-CDD congeners is more likely due to their dominant partition in particulate phases.

3.2. Reactions of PCDD-OH adducts with O_2

In the atmosphere, the PCDD-OH adducts would react with O_2 (Scheme S1) through combination to form peroxy radicals (Lee et al., 2004), hydrogen abstraction to form PCDD-β-ol for PCDD-β-OH as for benzene and dibenzofuran (Calvert et al., 2002; Altarawneh et al., 2008; Glowacki et al., 2009), and fused-ring C–O bond cleavage for the PCDD-γ-OH adducts to form substituted phenoxy radicals (Wang and Tang, 2011). Rate constants for combinations between PCDD-OH and O_2 were only recently available on 2,3,7,8-γ-OH from DFT and TST calculations by (Zhang et al., 2011). In our previous study on reactions of DD-OH and 2,3,7,8-TCDD-OH with O_2 (Wang and Tang, 2011), the rate constants were assumed to be similar to that of DF-OH + O_2 predicted by (Altarawneh et al., 2008). In current study, the reaction kinetics of PCDD-OH and O_2 is examined using DD-β/γ-OH as prototypes.

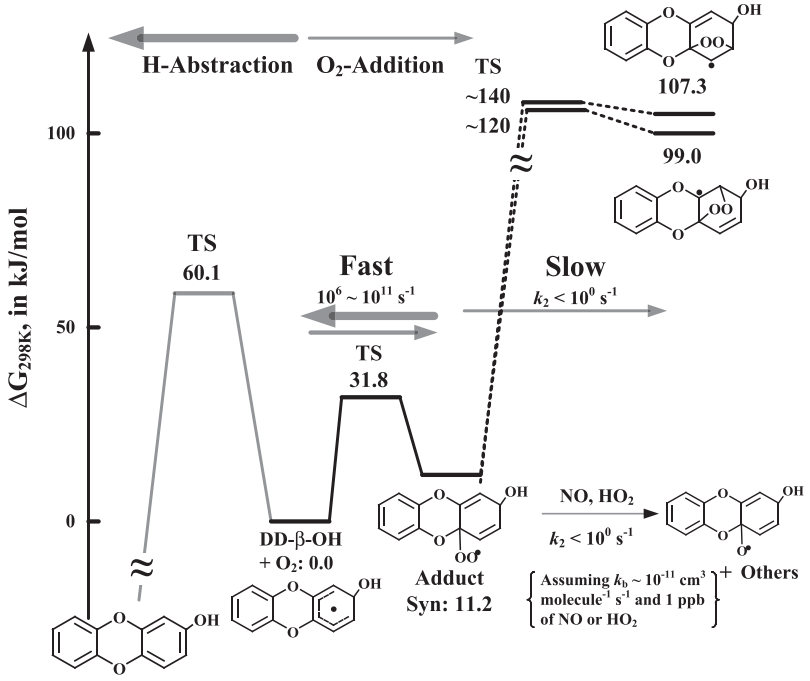

Fig. 2. The potential energy diagram for DD-β-OH + O_2 ($\Delta_r G_{298K}$, in kJ mol^{-1}).

The geometries of the products and transition states are optimized here at UB3LYP/6-311++G(2df,p) level for reactions between DD-β/γ-OH and O_2. It is noticed that the UB3LYP calculations on transition states for O_2 addition suffer from severe spin contamination with $<S^2> = 0.9 \sim 1.1$. This would lead to overestimation of the barrier heights, and would partially compensate the underestimation of B3LYP method (Zhao and Truhlar, 2005). It is desirable to calculate the reaction energetics at high levels of RCCSD(T)/6-311+G(2df,2p) or G3XMP2-RAD as for the reaction of C_6H_6-OH and O_2 in previous studies (Glowacki et al., 2009; Olivella et al., 2009). However, these methods are computationally too intensive for current DD-OH + O_2 system.

Table S3 shows a comparison between UB3LYP/6-311++G(2df,p) and the previous G3XMP2-RAD results on C_6H_6-OH + O_2 reaction (Glowacki et al., 2009), on which UB3LYP underestimates the exothermicity by 22 ~ 32 (average: 26.3) kJ mol^{-1} but overestimates the barrier heights by 14 ~ 16 (average: 15.6) kJ mol^{-1} for O_2-additions to C_6H_6-OH. For hydrogen abstraction from C_6H_6-OH, the UB3LYP barrier height is 3.4 kJ mol^{-1} lower than the G3XMP2-RAD one. The average deviations of UB3LYP to G3XMP2-RAD on C_6H_6-OH + O_2 are applied directly to DD-OH + O_2 (Table S3).

The rate constants for O_2 addition to DD-OH adducts can again be estimated using the traditional TST (Table S4). The overall $k_{b,298K}$ are 7.25×10^{-13} and 3.56×10^{-16} cm^3 mol^{-1} s^{-1} for O_2 additions to DD-β-OH and DD-γ-OH, respectively, being much higher than the values of $10^{-19} \sim 10^{-17}$ cm^3 mol^{-1} s^{-1} for C_6H_6-OH or DF-OH and O_2 (Altarawneh et al., 2008; Olivella et al., 2009), or the value of $10^{-21} \sim 10^{-20}$ cm^3 mol^{-1} s^{-1} for TCDD-γ-OH and O_2 (Zhang et al., 2011). The large $k_{b,298K}$ for DD-β-OH is due to the O_2 addition to C_{12} site where the transition barrier is low because the intramolecular H-bond formed between O_2 and –OH group.

Table 2
Reaction energetics (in kJ/mol) and high-pressure-limit rate constants (k_{Uni} in s^{-1}) for fused-ring C-O decompositions of PCDD-γ-OH adducts.

PCDD-γ-OH	$\Delta_r H_{0K}$	$\Delta_r G_{298K}$	$\Delta_r H_{0K}^{\ddagger}$	$\Delta_r G_{298K}^{\ddagger}$	k_{Uni} (s^{-1})
DD-11-γ-OH	−51.3	−58.3	46.9	47.0	3.57×10^4
1,4-DCDD-11-γ-OH	−43.9	−50.0	58.3	57.7	4.82×10^2
1,4-DCDD-14-γ-OH	−52.8	−60.3	43.6	43.6	1.45×10^5
1,6-DCDD-11-γ-OH	−40.6	−48.1	54.3	53.8	2.31×10^3
1,6-DCDD-12-γ-OH	−49.0	−63.3	48.1	48.1	2.33×10^4
1,9-DCDD-11-γ-OH	−50.0	−57.9	53.9	53.4	2.77×10^3
1,9-DCDD-12-γ-OH	−51.9	−57.9	47.5	47.4	3.12×10^4
2,3-DCDD-11-γ-OH	−53.5	−59.5	50.6	50.9	7.62×10^3
2,3-DCDD-14-γ-OH	−52.9	−60.0	45.2	45.0	8.13×10^4
2,7-DCDD-11-γ-OH	−60.6	−67.0	48.5	48.0	2.42×10^4
2,7-DCDD-12-γ-OH	−44.8	−51.6	47.2	47.5	2.93×10^4
2,8-DCDD-11-γ-OH	−51.5	−59.2	46.9	47.0	3.60×10^4
2,8-DCDD-12-γ-OH	−55.1	−61.1	48.8	48.9	1.67×10^4
1,4,6,9-TCDD-11-γ-OH	−47.3	−51.3	54.4	53.6	2.48×10^3
2,3,7,8-TCDD-11-γ-OH	−54.8	−61.0	49.1	48.8	1.77×10^4
OCDD-11-γ-OH	−47.3	−51.2	43.3	42.7	2.02×10^5

However, formation of DD-β/γ-OH-O_2 peroxy adducts is not the rate-determining step for removing DD-β/γ-OH from the atmosphere. Fig. 2 shows the Gibbs energy changes for the addition between DD-β-OH and O_2. Under the atmospheric conditions, the DD-OH-O_2 peroxy radicals would decompose back unimolecularly to DD-OH + O_2 rapidly at rates of $10^6 \sim 10^{11}$ s^{-1}; while the reactions with trace HO_2 or NO_x radicals are slow with rates <1 s^{-1}, assuming rate constants of ~10^{-11} cm^3 mol^{-1} s^{-1} between DD-OH-O_2 and NO_x or HO_x and the ambient concentrations of ~1 ppb for NO_x or HO_x (Calvert et al., 2008). The forward ring-closure isomerization as for C_6H_6-OH-O_2 (Calvert et al., 2002; Suh et al., 2003; Olivella et al., 2009) are also slow with rate <1 s^{-1} with high barriers. Therefore, quasi-equilibrium can be assumed between DD-OH + O_2 and DD-OH-O_2 adducts:

$$\text{DD-OH} + O_2 \underset{\text{Fast}}{\overset{K_{Equ}}{\rightleftharpoons}} \text{DD-OH} - O_2 \underset{\text{Slow}}{\overset{K_2}{\rightarrow}} \text{Products}$$

and the effective bimolecular rate constants ($k_{b,Eff}$) can be expressed as:

$$k_{b,Eff} = k_2 \cdot K_{Equ} = k_2 \cdot \frac{RT}{P^{\circ}} \cdot \exp\left(-\frac{\Delta_r G_{298K}}{RT}\right) \cdot \frac{10^6}{N_A} \quad \text{(E3)}$$

where k_2 is less than 1 s^{-1} as mentioned above, and $k_{b,Eff}$ is in cm^3 mol^{-1} s^{-1}. The $k_{b,Eff}$ for DD-OH and O_2 addition become 2.94×10^{-21} and 2.53×10^{-23} cm^3 mol^{-1} s^{-1} for DD-β-OH and DD-γ-OH (Table S4), respectively, rendering their negligible importance in the atmosphere. Alternatively, DD-β-OH will react with O_2 via direct hydrogen abstraction, forming DD-2-ol, with $k_b \sim 10^{-17}$ cm^3 molecule^{-1} s^{-1} and the rates, $k_b[O_2]$, of ~50 s^{-1}.

The slow reactions with O_2 imply that the PCDD-β-OH adducts may have chance to react directly with the atmospheric trace radicals such as NO_x and HO_x. The reactions with NO_x may lead to formation of nitrated PCDDs as for polycyclic aromatic hydrocarbons (Arey et al., 1986; Helmig et al., 1992; Atkinson and Arey, 1994), and may introduce carcinogenic toxicity different from PCDDs.

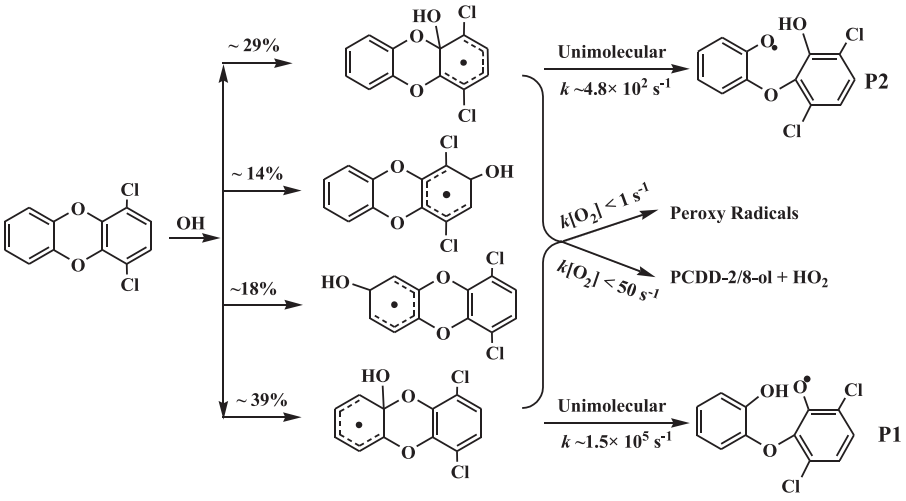

Scheme 1. The oxidation mechanism of 1,4-Di-CDD in the atmosphere.

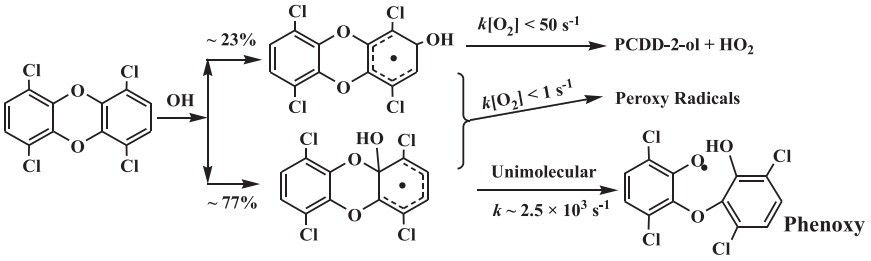

Scheme 2. The oxidation mechanism of 1,4,6,9-TCDD in the atmosphere.

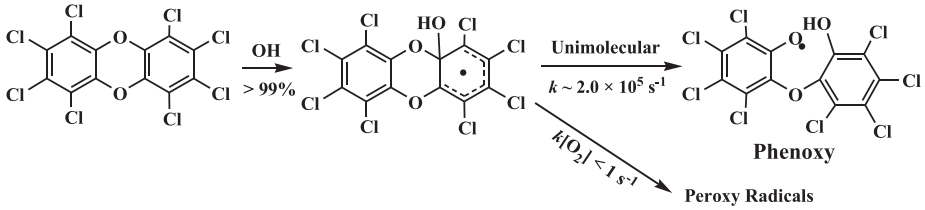

Scheme 3. The oxidation mechanism of Octa-CDD in the atmosphere.

3.3. Bond cleavages of PCDD-γ-OH adducts

Because of the negligible removal by O_2, PCDD-γ-OH adducts will undergo fused-ring C–O bond cleavage, forming the substituted phenoxy radicals. The transition barriers for such processes are below the initial reactants PCDD + OH (Fig. 1). Table 2 lists the reaction energetics, barrier heights, and the high-pressure-limit unimolecular rate constants for the fused-ring C–O bond cleavage processes of PCDD-γ-OH adducts. The bond cleavages occur at rates of $10^3 \sim 10^5\ s^{-1}$, being much faster than their reactions with the atmospheric O_2 (rates <1 s^{-1}). Therefore, C–O cleavage will dominate for all PCDD-γ-OH adducts. This is significantly different from the fate of PCDD-OH-β adducts. In contrast, a similar C–O bond cleavage for DF-OH adduct has barrier higher than DF + OH by about 50 kJ mol^{-1} (Altarawneh et al., 2008).

4. Conclusions

The atmospheric oxidation mechanism of PCDDs initiated by OH radical has been studied using DFT-B3LYP calculations. The oxidation is initiated by OH addition predominantly to the C_γ and non-chlorinated C_β sites; while the addition to C_α and chlorinated sites are negligible. In the atmosphere, the PCDD-β-OH adducts will react with O_2 to form PCDD-β-ols, while PCDD-γ-OH adducts will undergo fused-ring C-O breakage, forming substituted phenoxy radicals. The gas-phase oxidation products for 2,3,7,8-PCDDs will be the substituted phenoxy radicals with almost unit yield; while for PCDDs with non-chlorinated β-carbon, there will be a minor productions of PCDD-β-ol with yields in the range of ~10% for 2,7-DCDD to ~42% for DD. Typical atmospheric oxidation pathways of 1,4-Di-CDD, 1,4,6,9-TCDD, and Octa-CDD are summarized in Schemes 1–3, and Schemes S2 to S6 for others. In the atmosphere, the substituted phenoxy radicals do not reaction with O_2 (Platz et al., 1998), but do possibly react with other atmospheric radical species such as NO_x and HO_x, etc. Overall, the atmospheric oxidation mechanisms of PCDD initialized by OH radical are drastically different from those of benzene and dibenzofuran.

Acknowledgments

We thank for the service support of the high-performance computing platform SCUTGrid from Information Network Research and Engineering Centre of South China University of Technology and the financial supports from NSF China (20777017 and 21177041) and the Fundamental Research Fund for the Central Universities of China (2009ZM0176).

Appendix A. Supplementary material

Supplementary data associated with this article can be found, in the online version, at http://dx.doi.org/10.1016/j.chemosphere.2012.06.050.

References

Altarawneh, M., Kennedy, E.M., Dlugogorski, B.Z., Mackie, J.C., 2008. Computational study of the oxidation and decomposition of dibenzofuran under atmospheric conditions. J. Phys. Chem. A 112, 6960–6967.

Arey, J., Zielinska, B., Atkinson, R., Winer, A.M., Ramadahl, T., Pitts Jr., J.N., 1986. The formation of nitro-PAH from the gas-phase reactions of fluoranthene and pyrene with the OH radical in the presence of NO_x. Atmos. Environ. A 20, 2339–2345.

Atkinson, R., 2001. Atmospheric lifetimes of dibenzo-*p*-dioxins and dibenzofurans. Sci. Total Environ. 104, 17–33.

Atkinson, R., Arey, J., 1994. Atmospheric chemistry of gas-phase polycyclic aromatic hydrocarbons: formation of atmospheric mutagens. Environ. Health Perspect. 102 (4), 117–126.

Brubaker Jr., W.W., Hites, R.A., 1998. OH reaction kinetics of polycyclic aromatic hydrocarbons and polychlorinated dibenzo-*p*-dioxins and dibenzofuran. J. Phys. Chem. A 102, 915–921.

Bryukov, M.G., Knyazev, V.D., Gehling Jr., W.M., Dellinger, B., 2009. Kinetics of the gas-phase reaction of OH with chlorobenzene. J. Phys. Chem. A 113, 10452–10459.

Brzuzy, L.P., Hites, R.A., 1996. Global mass balance for polychlorinated dibenzo-*p*-dioxins and dibenzofurans. Environ. Sci. Technol. 30, 1797–1805.

Bylaska, E.J., de Jong, W.A., Kowalski, K., Straatsma, T.P., Valiev, M., Wang, D., Apra, E., Windus, T.L., Hirata, S., Hackler, M.T., et al., 2006. NWChem, a computational chemistry package for parallel computers, version 5.0: Pacific Northwest National Laboratory, Richland, Washington, USA, pp. 99352–0999.

Calvert, J.G., Atkinson, R., Becker, K.H., Kamens, R.M., Seinfeld, J.H., Wallington, T.J., Yarwood, G., 2002. The Mechanisms of Atmospheric Oxidation of the Aromatic Hydrocarbons. Oxford University Press.

Calvert, J.G., Derwent, R.G., Orlando, J.J., Tyndall, G.S., Wallington, T.J., 2008. Mechanisms of Atmospheric Oxidation of the Alkanes. Oxford University Press.

Chao, M.-R., Hu, C.-W., Chen, Y.-L., Chang-Chien, G.-P., Lee, W.-J., Chang, L.W., Lee, W.-S., Wu, K.-Y., 2004. Approaching gas-particle partitioning equilibrium of atmospheric PCDD/Fs with increasing distance from an incinerator: measurements and observations on modeling. Atmos. Environ. 38, 1501–1510.

Eitzer, B.D., Hites, R.A., 1988. Vapor pressures of chlotinated dioxins and dibenzofurans. Environ. Sci. Technol. 22, 1362–1364.
Frisch, M.J., Trucks, G.W., Schlegel, H.B., Scuseria, G.E., Robb, M.A., Cheeseman, J.R., Montgomery, J.J.A., Vreven, T., Kudin, K.N., Burant J.C., et al., 2004. Gaussian 03, Revision B.05. Wallingford, CT.
Glowacki, D.R., Wang, L., Pilling, M.J., 2009. Evidence of formation of bicyclic species in the early stages of atmospheric benzene oxidation. J. Phys. Chem. A 113, 5385–5396.
Handy, N.C., Cohen, A.J., 2001. O3LYP. Mol. Phys. 99, 403.
Helmig, D., Arey, J., Atkinson, R., Harger, W.P., McElroy, P.A., 1992. Products of the OH radical-initiated gas-phase reaction of fluorene in the presence of NO_x. Atmos. Environ. A 26, 1735–1745.
Hippelein, M., Kaupp, H., Dorr, G., McLachlan, M., Hutzinger, O., 1996. Baseline contamination assessment for a new resource recovery facility in Germany Part II: atmospheric concentrations of PCDD/F. Chemosphere 32, 1605–1616.
Hofzumahaus, A., Rohrer, F., Lu, K., Bohn, B., Brauers, T., Chang, C.-C., Fuchs, H., Halland, F., Kita, K., Kondo, Y., et al., 2009. Amplified trace gas removal in the troposphere. Science 324, 1702–1704.
Kaupp, H., McLachlan, M.S., 1999. Gas/particle partitioning of PCD/Fs. PCBs, PCNs and PAHs. Chemosphere 38, 3411–3421.
Kowk, E.S.C., Arey, J., Atkinson, R., 1994. Gas-phase atmospheric chemistry of dibenzo-*p*-dioxin and dibenzofuran. Environ. Sci. Technol. 28, 528–533.
Kowk, E.S.C., Atkinson, R., Arey, J., 1995. Rate constants for the gas-phase reactions of the OH radical with dichlorobiphenyls, 1-chlorodibenzo-p-dioxin, 1,2-dimethoxybenzene, and diphenyl ether: Estimation of OH radical reaction rate constants for PCBs, PCDDs, and PCDFs. Environ. Sci. Technol. 29, 1591–1598.
Lee, J.E., Choi, W., Mhin, B.J., Balasubramanian, K., 2004. Theoretical study on the reaction of OH radicals with polychlorinated dibenzo-p-dioxins. J. Phys. Chem. A 108, 607–614.
Lee, R.G.M., Green, N.J.L., Lohmann, R., Jones, K.C., 1999. Seasonal, anthropogenic, air mass, and meteorological influences on the atmospheric concentrrations of polychlorinated dibenzo-*p*-dioxins and dibenzofurans (PCDD/Fs): evidence for the importance of diffuse combustion sources. Environ. Sci. Technol. 33, 2864–2871.
Lee, S.-J., Ale, D., Chang, Y.-S., Oh, J.-E., Shin, S.K., 2008. Seasonal and particle size-dependent variations in gas/particle partitioning of PCDD/Fs. Environ. Pollut. 153, 215–222.
Li, H., Feng, J., Sheng, G., Lv, S., Fu, J., Peng, P.a., Man, R., 2008a. The PCDD/F and PBDD/F pollution in the ambient atmosphere of Shanghai, China. Chemosphere 70, 576–583.
Li, Y., Jiang, G., Wang, Y., Cai, Z., Zhang, Q., 2008b. Concentrations, profiles and gas-particle partitioning of polychlorinated dibenzo-*p*-dioxins and dibenzofurans in the ambient air of Beijing. China. Atmos. Environ. 42, 2037–2047.
Lohmann, R., Green, N.J.L., Jones, K.C., 1999. Atmospheric transport of polychlorinated dibenzo-*p*-dioxins and dibenzofurans (PCDD/Fs) in air mass across the United Kingdom and Ireland: Evidence of emissions and depletion. Environ. Sci. Technol. 33, 2872–2878.
Lohmann, R., Lee, R.G.M., Green, N.J.L., Jones, K.C., 2000. Gas-particle partitioning of PCDD/Fs in daily air samples. Atmos. Environ. 16, 2529–2537.
Mader, B.T., Pankow, J.F., 2003. Vapor pressures of the polychlorinated dibenzodioxins (PCDDs) and the polychlorinated dibenzofurans (PCDFs). Atmos. Environ. 37, 3103–3114.
Nakano, T., Tsuji, M., Okuno, T., 1990. Distribution of PCDDs, PCDFs and PCBs in the atmosphere. Atmos. Environ. 24A, 1361–1368.
Ohura, T., Fujima, S., Amagai, T., Shinomiya, M., 2008. Chlorinated polycyclic arpmatic hydrocarbons in the atmosphere: seasonal levels, gas-particle partitioning, and origin. Environ. Sci. Technol. 42, 3296–3302.
Olivella, S., Sole, A., Bofill, J.M., 2009. Theoretical mechanistic study of the oxidative degradation of benzene in the troposphere: Reaction of benzene-HO radical adduct with O_2. J. Chem. Theory Comput. 5, 1607–1623.
Pilling, M.J., Seakins, P.W., 1999. Reaction Kinetics. Oxford University Press Inc., New York.
Platz, J., Nielsen, O.J., Wallington, T.J., Ball, J.C., Hurley, M.D., Straccia, A.M., Schneider, W.F., Sehested, J., 1998. Atmospheric chemistry of the phenoxy radical, C_6H_5O: UV spectrum and kinetics of its reaction with NO, NO_2, and O_2. J. Phys. Chem. A 102, 7964–7974.
Shih, M., Lee, W.-S., Chang-Chien, G.-P., Wang, L.-C., Hung, C.-Y., Lin, K.-C., 2006. Dry deposition of polychlorinated dibenzo-*p*-dioxins and dibenzofurans (CPDD/Fs) in ambient air. Chemosphere 62, 411–416.
Sinkkonen, S., Paasivirta, J., 2000. Degradation half-life times of PCDDs, PCDFs and PCBs for environmental fate modeling. Chemosphere 40, 943–949.
Song, Y., Qian, X.-M., Lau, K.-C., Ng, C.Y., Liu, J., Chen, W., 2001. High-resolution energy-selected study of the reaction CH3X+ → CH3+ + X: Accurate thermochemistry for the CH3X/CH3X+ (X = Br, I) system. J. Chem. Phys. 115, 4095–4105.
Suh, I., Zhang, R., Molina, L.T., Molina, M.J., 2003. Oxidation mechanism of aromatic peroxy and bicyclic radicals from OH-toluene reactions. J. Am. Chem. Soc. 125, 12655–12665.
Taylor, P.H., Yamada, T., Neuforth, A., 2005. Kinetics of OH radical reactions with dibenzo-p-dioxin and selected chlorinated dibenzo-p-dioxins. Chemosphere 58, 243–252.
Tokmakov, I.V., Lin, M.C., 2002. Kinetics and mechanism of the OH + C_6H_6 reaction: a detailed analysis with first-principles calculations. J. Phys. Chem. A 106, 11309–11326.
Valsaraj, K.T., Thibodeaux, L.J., 2010. On the physicochemical aspects of the global fate and long-range atmospheric transport of persistent organic pollutants. J. Phys. Chem. Lett. 1, 1694–1700.
Wang, L., Tang, A., 2011. Atmospheric oxidation mechanisms of polychlorinated dibenzo-*p*-dioxins are different from those of benzene and dibenzofuran: a theoretical study. Chemosphere 82, 782–785.
Zhang, C., Sun, T., Sun, X., 2011. Mechanism for OH-initiated degradation of 2,3,7,8-Tetrachlorinated dibenzo-*p*-dioxins in the presence of O_2 and NO/H_2O. Environ. Sci. Technol. 45, 4756–4762.
Zhang, Q., Qu, X., Wang, H., Xu, F., Shi, X., Wang, W., 2009. Mechanism and thermal rate constants for the complete series reactions of chlorophenols with H. Environ. Sci. Technol. 43, 4105–4112.
Zhao, Y., Truhlar, D.G., 2005. Design of density functionals that are broadly accurate for thermochemistry, thermochemical kinetics, and nonbonded interactions. J. Phys. Chem. A 109, 5656–5667.